Arch. Metall. Mater. **67** (2022), 4, 1217-1226

DOI: https://doi.org/10.24425/amm.2022.141045

V. BHUVANESWARI[1], L. RAJESHKUMAR[1*], R. SARAVANAKUMAR[2], D. BALAJI[1]

SYNTHESIS AND CHARACTERIZATION OF BIOCERAMICS REINFORCED ALUMINIUM MATRIX COMPOSITES

Current work attempts to fabricate aluminium alloy AA2219 metal matrix composite (AMC) reinforced with natural bio-based sea shell powder (SSP) which is a ceramic material, in view of improving the mechanical and tribological properties. SSP was characterized by X-Ray Diffraction (XRD) to assess its chemical constituents and particle size. Stir casting route was adopted for fabricating AMCs reinforced with 1, 2 and 3 wt. % of SSP. Energy Dispersive X-ray Spectroscopy (EDS) was used to analyse the formation of secondary elements during casting and scanning electron microscopy (SEM) was used analyze the surface morphology of the composite specimen before and after tribological tests. Hardness, Compressive strength and tribological properties were evaluated using appropriate tests and corresponding ASTM standards. Characterization methods revealed that the formation of secondary elements was very low at 3 wt. % of SSP when compared with other compositions. Hardness and compressive strength was found to be maximum for 3 wt. % of SSP while the specific wear rate and coefficient of friction values were found to be lesser for the same composite when compared with the unreinforced alloy and were on par with the AA2219 composites containing synthetic reinforcements.

Keywords: Metal matrix composites; Bioceramics; Hardness; Compressive strength; wear rate

1. Introduction

Blending of more than two materials in order to obtain enhanced properties, when compared with the monolithic materials, results in formation of composites. Composite materials are commonly categorised as Metal, Polymer and Ceramic Matrix Composites. Polymer composites are limited to light weight applications. Ceramic Matrix Composites is suitable for high temperature applications with intricacy in production and hence their processing would be comparatively expensive. Metal matrix composites provide high strength, fracture toughness, better resistance towards corrosion and wear at higher temperature when compared with polymer composites. Normally, metals like copper, aluminium and magnesium are used as matrix materials as they possess high strength and high modulus, better specific strength of resulting composites that are comparatively better than the monolithic alloys for majority of the applications. Vital application of AMCs includes automotive and thermal applications and many mechanical components like brake disc and piston. Owing to positive variation in mechanical properties, which depends on the reinforcement proportion and chemical composition of base metal, AMCs has been proven successful in various areas including functional and structural applications [1]. Few experimenters stated that attention was shown towards AMCs to a larger extent due to the benefits such as better strength, high wear resistance and hardness of end products [2]. AMCs can have reinforcements like silicon carbide and alumina which are the extensively used dispersion materials because of their extensive characteristics like high hardness and lesser wear rate [3]. When the dispersion is graphite, resulting composite possess less casting defects and appreciable surface finish [4]. Aluminium alloys, when used as matrix, has gained the focus of the material researchers due to various other salient characteristics like appreciable damping ability [5].

Some authors described that AA2219-Al_2O_3 nano composites developed by stir casting has shown improved mechanical properties [6]. Aluminium matrix composites containing alumina as reinforcement revealed an enhanced strength over the unreinforced alloys but reduced fracture toughness and ductility [7]. In contrast, monolithic alloys has better fracture toughness but are not widely preferred due to their low specific strength and stiffness [8-10] as these two properties play a significant role in prevention of failure of components subjected to impact loads and in-service stress [11,12]. For demand in cutting edge

[1] KPR INSTITUTE OF ENGINEERING AND TECHNOLOGY, DEPARTMENT OF MECHANICAL ENGINEERING, COIMBATORE – 641407, TAMILNADU, INDIA
[2] VSB COLLEGE OF ENGINEERING AND TECHNICAL CAMPUS, DEPARTMENT OF MECHANICAL ENGINEERING, COIMBATORE – 642109, TAMILNADU, INDIA

* Corresponding author: lrkln27@gmail.com

engineering applications, aluminium hybrid composites are used due to the result of better mechanical properties [13]. Production of hybrid reinforced AMCs reduces the processing cost of single reinforced MMCs [14, 15]. Derived ceramics including tungsten carbide, alumina, silica, silicon carbide, graphite and carbon nanotubes are broadly used in aluminium matrix and among them alumina and silicon carbide are frequently used when compared with other reinforcements [16]. Hybrid synthetic reinforcing particulates such as Graphite and Boron carbide are used for property optimization by adopting different design concepts in AMCs. Cost of synthetic reinforcements are high due to its unavailability in most developing countries. But the difficulties of high processing cost are not represented due to accomplishment of enhanced properties [17,18].

Research has been carried out for using the ceramic materials as reinforcements with alloys of aluminium to enhance the properties and tailoring them as per the application requisite in the field of industry and commercial areas [19]. Stir casting is the frequently used process of fabricating AMMCs during the recent days. Different methods were adopted to fabricate composites includes mechanical alloying, squeeze casting and stir casting [20]. Stir casting renders better strength to the AMCs and a strong interfacial bond is established between reinforcement and matrix by means of mutual dissolution of the elements at the time of casting. Because of this reason, good wettability of the dispersoids is much needed in stir casting process. Considering these facts, stir casting process is used for fabricating AMCs as it renders prolonged surface reaction between matrix and dispersoids [21,22]. Due to flexibility, simplicity and low cost, stir casting stands out as a widely accepted process. Because of less processing cost for mass production of MMCs, a weight proportion of up to 30 % of reinforcement can be accommodated by this process, resulting in superior bonding. The 2000 family of aluminium alloys have copper as the main alloying constituent and this series is known for its ability to be heat treated and high strength. Aluminium alloy AA2219 has a broad spectrum of application in defence, automobile and aircraft and is specifically used as brake pads and clutch plates in automobiles. Due to some appreciable properties like good weldability and easy machinability, aluminium alloy AA2219 is chosen as matrix [23].

Utilization of aluminium based alloys in contact applications was very limited due to its softer ductile nature [24]. Many researchers determined that upon suitable reinforcements, the wear resistance of the aluminium alloys could be enhanced. Few authors determined the wear resistance of AA2219 aluminium alloys reinforced with alumina and rice husk ash (RHA). When the content of was kept constant and the content of alumina was varied in between 1 wt. % and 3 wt. %, the wear resistance was found to increase along with it [25-27]. Few other experimental trials were carried out to determine the wear resistance of aluminium alloys reinforced with self-lubricating reinforcements like graphite and molybdenum-disulphide. From the experimental results, it was noted that there was a significant increase in the wear resistance of the aluminium alloys but at the cost of reduced mechanical properties. It was stated by the authors that when the proportion of self-lubricating materials was increased beyond 3 wt. %, mechanical properties drastically reduced [28]. Researches are ongoing to have enhanced mechanical and tribological properties simultaneously with the same reinforcement but only limited synthetic ceramics served the purpose. Even though it was achieved by few experimenters, the cost of manufacturing of composites were very high. Hence explorations has to be made in such a way that the composites renders better mechanical and tribological properties simultaneously at a cost-effective manufacturing process [29-31]. With all the above facts in mind, current work focusses on manufacturing AA2219 composites containing seashell powder (SSP) which is a natural bio-ceramic material through stir casting process. XRD and EDS were adopted to characterize the sea shell powder for its chemical constituents, particle size and secondary element formation.. Mechanical properties like hardness and compressive strength were evaluated for AA2219-SSP composites and were compared with AA2219-alumina composites to have a better evaluation of bio-based MMC. Tribological properties of the composites were determined using wear tests and the wear surface morphology of the composite specimens were characterized using SEM analysis.

2. Experimental work

2.1. Materials and methods

AA2219 was procured in the form of a billet in M/s RSA Metals Corporation, Coimbatore. Sea shell powder is utilized as reinforcement because of its high strength, for obtaining improved mechanical properties and is acquired from shores of marina beach. Its availability is abundant and collection was also simple. The collected powders were crushed manually to obtain coarse grained powders. In order to homogenize the particle size of SSP, they were ball milled for 3 hours with a ball-to-powder ratio of 10.1:1 and toluene was used as a process control agent. The ball milled powders were reinforced in different weight proportions such as 1, 2 and 3% in AA2219 matrix. Alumina powders (Avg. particle size – 30 μm) were purchased from M/s Rajalakshmi Scientific, Coimbatore, TN. General properties of AA2219 are listed in TABLE 1 and chemical constituents in AA2219 are listed in TABLE 2. Since sea shell powder is a novel, natural and bio-based reinforcement, its properties are yet to be evaluated.

TABLE 1

Physical Properties of AA2219*

Properties	Values
Density (g/cm^3)	2.84
Hardness (BHN)	28-30
Modulus of Elasticity (kN/mm^2)	73-76
Thermal conductivity (W/mK)	116-121
Melting Point (°C)	543-643

* ASM Material data sheet

TABLE 2

Chemical constituents in AA2219 [11]

Constituent	Cu	Fe	Mn	Si	Ti	V	Al
Proportion (%)	5.8	0.25	0.4	0.17	0.1	0.16	Bal

2.2. Process of composite manufacturing

Stir casting is a molten state process used for producing cast samples of AMCs and the setup is illustrated in Fig. 2. In this method, the matrix is mixed with reinforcement through stirring by mechanical means. The process involves mixing of both the materials in two steps: first, melting the AA2219 matrix by heating it at about 800°C in a ceramic crucible. Meanwhile the seashell powder, which was crushed to near fine powder form, is preheated to 350°C for a time period of 30 min. Second, the reinforcement, that was already heated, is dispersed in molten AA2219 matrix and is stirred constantly at 400 rpm for a time period of 8 min. Composite samples were prepared by reinforcing 1, 2 and 3 wt. % of seashell powder separately in AA2219 by adopting the aforementioned procedure. The cast is then taken out after allowing to cool at ambient conditions. Three composite samples with alumina as reinforcement was also prepared by adopting the aforementioned procedure.

2.3. X-Ray Diffraction

XRD was adopted to test the SSP with respect to the elemental constituents present in it along with the crystal structure. It is a commonly used non-destructive process (NDT) for evaluating the lattice structure of a material in solid, liquid or fluid form in terms of the peaks obtained. These peaks can be correlated with the standard peaks (usually JCPDS peaks) for confirming the elemental present. One more functionality of XRD technique is to characterize the powders for their particle size based on the peaks obtained. In the current work, a sample of 100 mg of sea shell powder was characterized by XRD. Standard practices were used for the XRD analysis. While carrying out the test, the samples were held rigid and the X-ray tubes rotated from 10° to 90° with a scanning range of 10°/min. The values obtained from the XRD analyses were used to calculate the particle size of the sea shell powder. The calculations were based on the Williamson- Hall equation, as given in equation (1) [27].

$$\beta \cos\theta = \frac{k\lambda}{t} + 4\varepsilon \sin\theta \tag{1}$$

where $k = 0.5$ (shape factor), $\lambda = 0.1539$ nm (X-ray wavelength). A plot between $\beta \cos\theta$ (ordinate) and 4 sin θ (abscissa) would render a straight-line equation in which the slope (m) could be equated to the lattice strain directly and the intercept (c) from which grain size (t) can be obtained by using the equation $c = k\lambda / t$.

2.4. Energy Dispersive Spectroscopy (EDS) analysis

EDS is also a NDT method that can render the chemical constituents present in the composite sample by measuring the variation of the energy levels within the sample which is obtained as a result of focusing the electron beam. Specifications given out by EDS may range between 1 to 2 microns from the surface. Hence this technique can be used to identify the various elements present in the cast AA2219-SSP and can also be used to examine the formation of secondary elements in the cast composite. Samples of size 15 × 15 × 15 mm was used to perform EDS analysis and the samples were polished using silicon carbide emery paper and were surface cleaned to make the sample devoid of dirt and other foreign bodies.

2.5. Mechanical properties

Hardness of the composites are usually measured using Brinell, Rockwell or Vickers Testing method. For metal matrix composite, Brinell hardness testing method is suitable because the cast products may be inhabited with coarse grain structure. In the current experiment, Brinell hardness test was used to evaluate the hardness values. A cubical specimen of dimensions 15 × 15 × 15 mm was prepared as per ASTM E10 standard and before testing the samples were polished using a 600 grit emery paper. The test was carried out under a load of 250 N and with a steel ball intender of diameter 5 mm and the holding time was maintained as 10 min for all the samples. Each specimen was subjected to three experimental trials and the average value was taken as the final value. Compression tests were carried out in a hydraulic operated universal testing machine (Make: Shimadzu) by following ASTM E9 standards. Dimension of the specimen was maintained as φ15 mm × 25 mm and the tests were carried out at room temperature. For both of the above tests, a total of three samples were taken in each composition and the average value has been used.

2.6. Tribological properties

Wear rate and coefficient of friction of AA2219-SSP samples were determined by performing tribological tests using a Pin-on-Disc wear testing equipment. Tests were carried out at ambient conditions as per ASTM G99 standards and the specimen were maintained with a circular cross section of dimensions 10 mm diameter and 30 mm height. In earlier literature, various input parameters like applied load in N, sliding distance in m, sliding velocity in m/s, speed in rpm and time of wear in seconds were considered. Reponses from the current experiments were specific wear rate in mm^3/Nm and coefficient of friction. Since the predominant use of aluminium alloys are in brake pad applications, the input parameters were taken in such a way that it replicates the practical conditions to a certain extent. In the

current experiments, the parameters considered were load (= 19.62 N), speed (= 800 rpm) and sliding distance (= 2000 m) [15, 22]. Based on the above parameters, time of wear was calculated to be 3.61 minutes and sliding velocity 9.22 m/s. Each specimen was subjected to wear twice and the average of both the values were finally considered.

2.7. Scanning Electron Microscope

SEM is majorly used to sweep a specific area on the surface and may reveal the sample microstructure at larger magnifications by focusing a smaller diameter primary electron beam upon this surface. Electron beam, when focused on such a small area, depicts the constituents in the sample along with their abundance. The study of microstructure of materials is a salient parameter for relating the mechanical, tribological and other characteristics of the composites with the effects of reinforcement additions [24]. In the current work, SEM was used to analyse the surface morphology of AA2219-SSP composites before and after subjecting the specimen to wear tests.

3. Results and discussion

3.1. Characterization of SSP

3.1.1. XRD analysis of SSP particles

The particle size of the sea shell powder was determined by XRD which can also throw some light upon the influence of particle size on the composite characteristics. Study of XRD peaks rendered the constituents of sea shell powder. The major constituents of sea shell powder are Calcium Carbonate (77%) with the crystal structure of rhombohedra and Calcium Hydroxide (59%) with the hexagonal crystal structure according to JCPDS 47-1743 [25,32]. Fig. 1 shows the XRD peaks of sea shell powder. It could be observed from the figure that majority of the peaks denote the presence of calcium hydroxide and calcium carbonate in the SSP and the presence of other elements was very rarely noticed. TABLE 3 shows the various peak positions and corresponding full width at half maximum (FWHM) values for the sea shell powder. These values were substituted in Williamson-Hall equation as stated earlier and the plot was made in between $\beta \cos\theta$ and 4 sin θ. From the obtained graph, the value of particle size of the SSP was obtained as 15.7 microns. Since the SSP was powdered only using a compact ball mill vial, deeper powder characterization using SEM could not be carried out at this stage.

TABLE 3

XRD Peak Values of SSP

S. No	Pos. [deg]	Peak Height [cm]	FWHM	d-spacing [Å]	Rel. Int. [%]
1	29.4273	21977.8	0.1092	3.03281	100
2	29.5123	11686.7	0.0312	3.03178	53.18
3	47.5192	4500.06	0.0936	1.91188	20.48
4	48.5248	3669.35	0.1092	1.87459	16.7
5	39.4176	3356.07	0.1248	2.28413	15.27
6	34.1273	3332.73	0.1092	2.62512	15.16

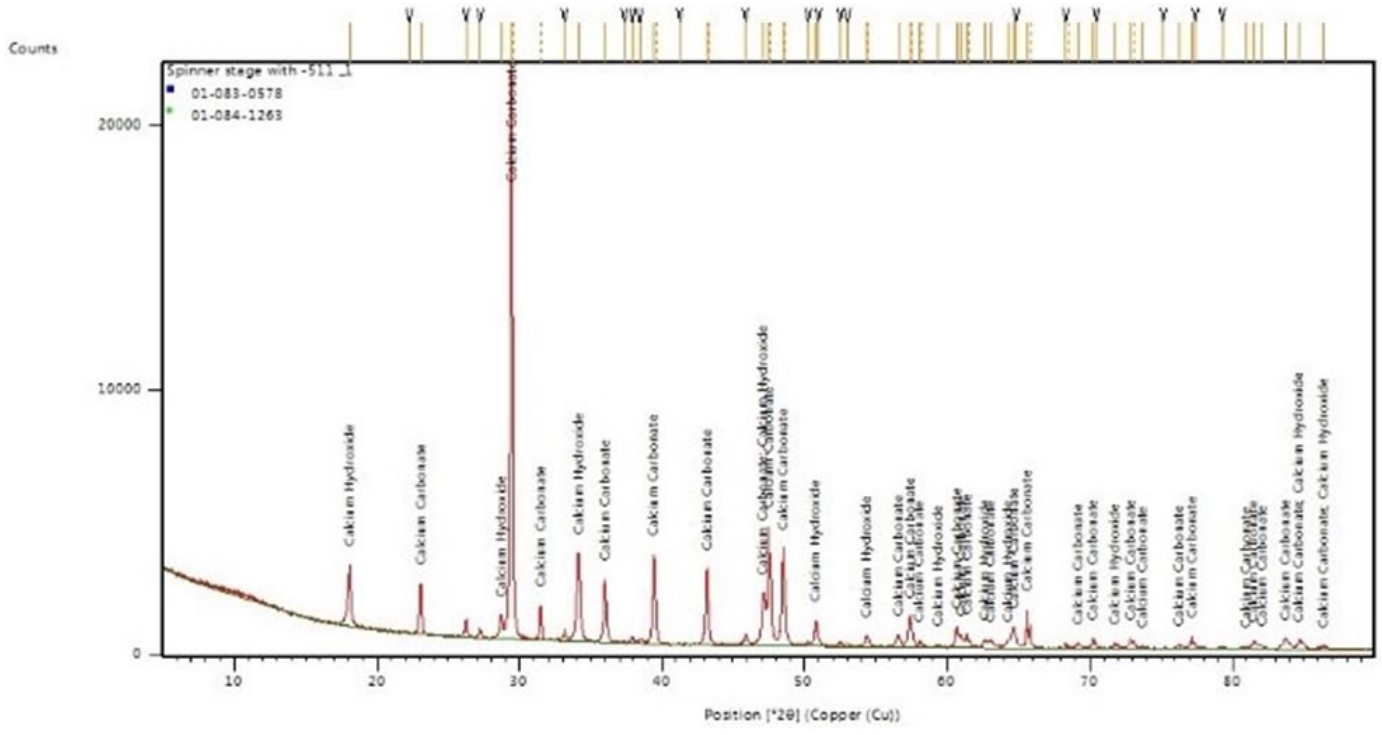

Fig. 1. XRD Peaks of sea shell powder

3.1.2. EDS analysis

Figs 2a-c shows the EDS images of AA2219-SSP composites with 1, 2 and 3 wt. % of SSP respectively. From the image presence of aluminium (Al), oxygen (O), carbon (C), copper (Cu) and calcium (Ca) were observed in the sample, endorsing the combined occurrence of AA2219 and SSP. It is evident from the spectral images that the peaks corresponding to aluminium is of maximum height while the peaks corresponding to copper and silicon is at a height next to Al peaks which conforms to the chemical composition of AA2219 as represented in TABLE 2. Since AA2219 is constituted with copper and silicon as second major alloying elements in terms of volume, the EDS peaks of both these elements were prominently observed for all compositions. Other elements such as O and Ca are the constituents of sea shell powder which are also prominently observed in the EDS spectra. From the spectra, it could be noted that hydrogen, which is also a constituent of SSP, is absent. It may be due to the fact that calcium hydroxide was decomposed, at higher temperatures, into calcium, oxygen and hydrogen while hydrogen reacted with the existing oxygen to form water that had evaporated. Silicon and copper atoms would have formed their respective oxides

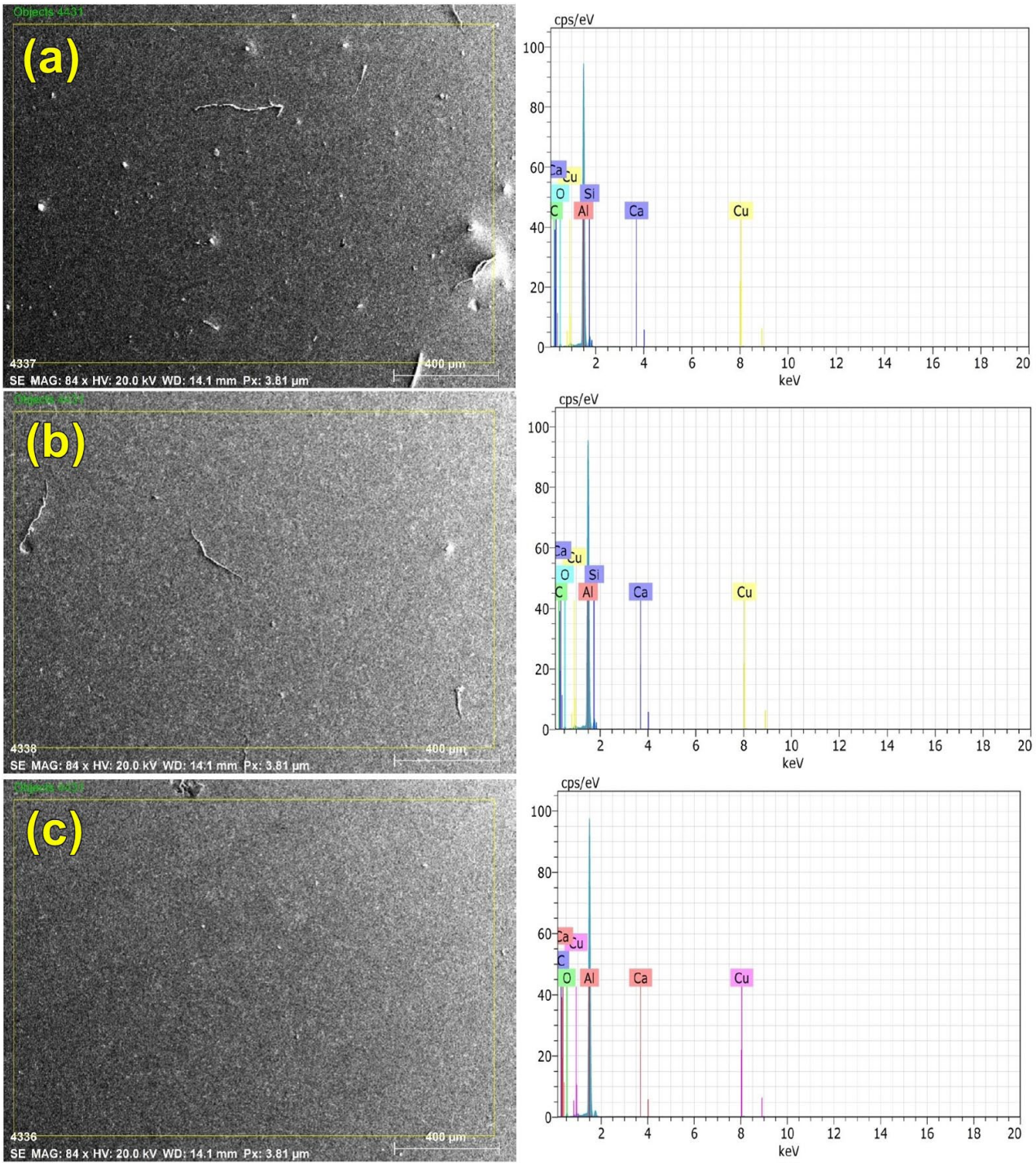

Fig. 2. EDS elemental mapping of AA2219 with a) 1 wt.% SSP, b) 2 wt. % SSP, c) 3 wt. % SSP

by combining with oxygen which were considered to be the secondary elements. Influence of these secondary elements was very less in the properties of resultant composites.

Distribution of various elements within each sample is listed in TABLE 4 for all the compositions of AA2219-SSP composites. Presence of C in the first EDS spectra is noticed to be high in Fig. 2a and subsequently reduces in the EDS spectra of other two samples as in Fig. 2b and 2c. Presence of carbon could be due to the conversion of aluminium atoms into carbon at higher temperatures than the melting point of aluminium. As the weight fraction of AA2219 reduces, the presence of carbon has also gradually reduced in the EDS spectra. Similarly presence of oxygen is observed to be high in Fig. 2b and 2c, which could possibly be due to the oxidation of Si and Cu resulting in the formation of their respective oxides. Presence of Ca was noted to be almost constant in all the three samples which could be due to the degradation of SSP which contains calcium carbonate and calcium hydroxide at higher temperatures. Calcium carbonate has disintegrated into calcium oxide and carbon dioxide at higher temperatures which is evidently witnessed in the EDS spectra. From the EDS surface mapping, it was observed that the increase in content of sea shell powder has reduced the porosity of the base metal and rendered a uniform surface for AA2219-SSP composites. Hence it could be stated that, the presence of 3 wt. % of SSP in AA2219 results in better microstructure with lesser amount of secondary elements formation.

TABLE 4

Elemental composition based on EDS analysis

AA2219 + 1 wt. % SSP		AA2219 + 2 wt. % SSP		AA2219 + 3 wt. % SSP	
Element	**wt.%**	**Element**	**wt.%**	**Element**	**wt.%**
Aluminium	74.98	Aluminium	73.91	Aluminium	67.06
Carbon	17.50	Carbon	16.42	Carbon	21.87
Copper	2.97	Copper	2.70	Copper	2.49
Oxygen	2.32	Oxygen	4.13	Oxygen	5.10
Silicon	1.02	Silicon	1.04	Silicon	1.12
Calcium	0.74	Calcium	1.32	Calcium	2.04
Magnesium	0.43	Magnesium	0.39	Magnesium	0.26

3.2. Mechanical Properties of AA2219-SSP composites

3.2.1. Effect of SSP addition on Hardness

Hardness test results of AA2219-SSP composites are tabulated in TABLE 5 and are compared with the hardness tests results of AA2219-alumina composites. Results show that the sample containing 3 wt. % of sea shell powder has the highest hardness value among all other samples. Hence the value of hardness increases with the increase in content of SSP. This could be attributed to the inherent property of ceramic particles presence within AA2219 matrix. Further, as the SSP is harder than alumina particles, the values of hardness is higher for each composite sample. It could also be stated that the value of hardness increases when the localized resistance of composites towards the indentation increases with the increase in weight fraction of SSP. Hardness values could also be attributed to the agglomeration of SSP within the matrix which reduced with the increase in content of SSP and so the hardness of the samples increased. Even though the sea shell powder is a brittle ceramic material, it enhanced the mechanical property of the pure matrix material to an appreciable extent. Fig. 3 depicts the variation of hardness values with the weight fractions of SSP and alumina in AA2219 matrix along with the error values.

TABLE 5

Hardness test result

Sample	Weight fraction (wt. %)	Hardness of AA2219-SSP (HB)	Hardness of AA2219-Al_2O_3 (HB)
1	0	28.62 ± 1.05	28.85 ± 1.15
2	1	29.57 ± 1.28	23.68 ± 1.39
3	2	39.13 ± 1.35	28.84 ± 2.14
4	3	48.5 ±1.24	34.43 ± 1.84

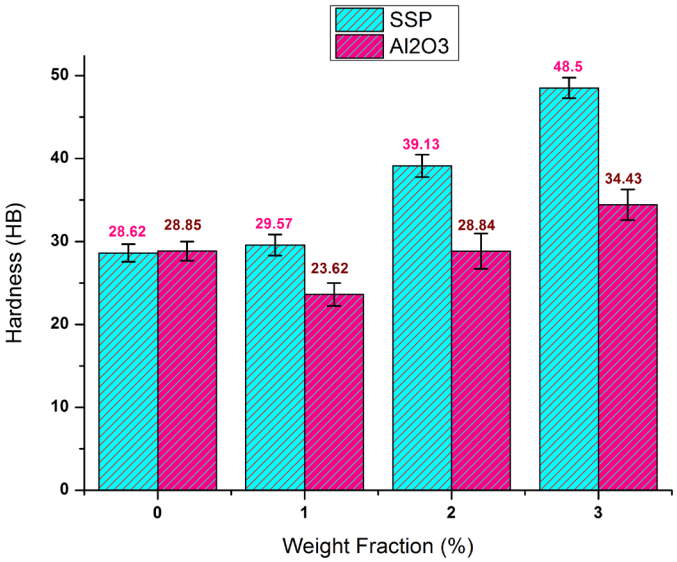

Fig. 3. Variation of hardness of AA2219 composites with SSP and alumina

3.2.2. Effect of SSP addition on compression strength

Compressive strength values of AA2219-SSP are tabulated in TABLE 6 and are compared with the strength of AA2219-Al_2O_3 samples. Fig. 4 depicts the variation of compressive strength with the weight fraction of SSP and alumina along with the error values. Values show that the compression strength of the composites linearly increase with the content of reinforcements and the maximum value is attained at 3 wt. % for both the reinforcements. Better compressive strength for the composite sample with highest weight fraction of reinforcement is due to the homogenous distribution of reinforcements within AA2219

matrix. This has, in turn, reduced the movement of dislocations during compressive loading of the composites and hence the strength of the sample attained is maximum.

TABLE 6

Compression test results

Sample	Weight fraction (wt. %)	Compressive strength of AA2219-SSP (MPa)	Compressive strength of AA2219-Al_2O_3 (MPa)
1	0	140 ± 2.7	140 ± 2.5
2	1	151.6 ± 2.9	149.1 ± 2.2
3	2	163.2 ± 3.2	158.2 ± 1.8
4	3	174.8 ± 2.5	167.3 ± 3.1

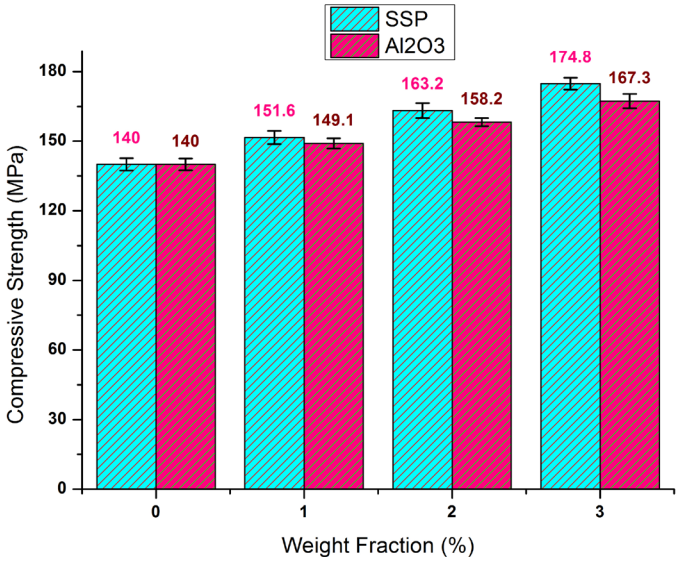

Fig. 4. Variation of compressive strength of AA2219 composites with SSP and alumina

Since the increase in SSP content decreased the space within the particles in a specific area, the stress transfer has not directly occurred in the base metal and the resistance of AA2219 towards deformation has increased due to the presence of SSP. Meanwhile, the compressive strength of SSP is noted to be on par with the alumina samples which shows that SSP, a bio-ceramic, could act as a potential substitute for most of the applications where synthetic ceramics are currently used. From the above studies, it could be concluded that AA2219 composites with 3 wt. % of SSP renders better mechanical performance when compared with all other compositions and other equivalent synthetic ceramics.

3.3. Tribological Properties of AA2219-SSP composites

Fig. 5 depicts the variation of specific wear rate of AA2219-seashell powder composites with the weight fraction of seashell powder. TABLE 7 depicts the effect of sea shell powder addition upon the specific wear rate and coefficient of friction. It could be observed from the table that variation of specific wear rate is directly proportional to the variation of SSP content while the variation of coefficient of friction is inversely proportional to the content of SSP. Since the dispersion of SSP is homogenous within AA2219 at 3 wt. %, the specific wear rate was found to be minimum. This could possibly due to the fact that during wear, SSP first comes into contact with the counterfacing disc thus shielding the softer matrix material from wear loss. Hence, the specific wear rate was relatively lower at this composition. At all other previous compositions, due to non-homogenous distribution of seashell powder and poor interfacial adhesion between AA2219 and seashell powder, the reinforcement might had slipped from the matrix thus exposing the softer matrix to the counterfacing disc. This resulted in higher specific wear rates for the composites with 1 and 2 wt. % of seashell powder. These values were significantly supported by the coefficient of friction values which decreases with the increase in content of seashell powder. Hardness values of the composite materials substantiate the variation of specific wear rate of the composite samples. As the composite with 3 wt. % of SSP was harder, it exhibited lowest specific wear rate and this phenomenon is applicable to all other specimens. Hence it could be concluded that AA2219 composites with 3 wt. % of seashell powder had higher wear resistance when compared with other compositions.

TABLE 7

Wear test result

Sample	Weight fraction (wt. %)	Applied load (N)	Speed (m/s)	Sliding Distance (m)	Wear loss (mm^3/N.m)	Coefficient of Friction
1	0	19.62	800	2000	2.04×10^{-13}	0.273
2	1	19.62	800	2000	1.92×10^{-13}	0.166
3	2	19.62	800	2000	1.56×10^{-13}	0.152
4	3	19.62	800	2000	1.32×10^{-13}	0.097

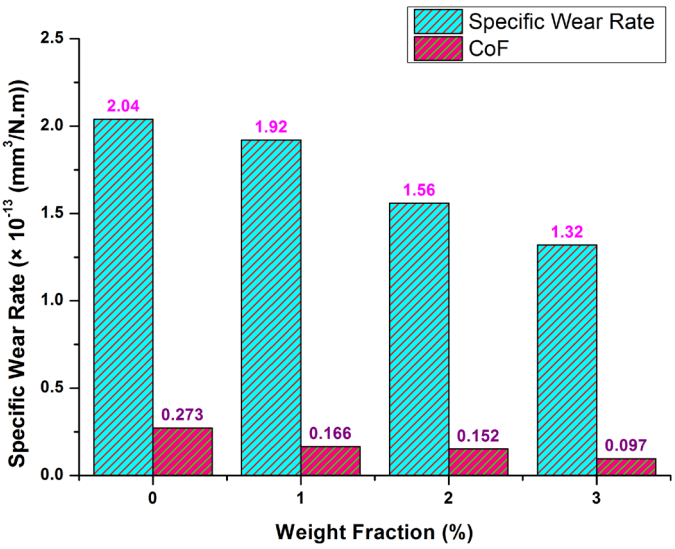

Fig. 5. Variation of wear rate and coefficient of friction with SSP content

3.4. Surface Morphology of AA2219-SSP composites

Surface morphology of AA2219-SSP composites before and after wear test was analyzed using SEM. Fig. 6 shows the SEM images of AA2219-SSP composites before and after wear tests. From Fig. 6(a) it could be noted that the surface exhibits few casting defects and the agglomerated reinforcements. This clearly portrays the inadequacy of SSP powders present in the sample to get homogenously dispersed within the matrix and the closely packed atoms in hexagonal crystal structure of the reinforcement. Normally stirring condition and preheating of reinforcement at the time of fabrication determines the property of the AA2219-SSP composites [11]. It could be seen from the image that SSP powder has been agglomerated in spite of preheating before mixing with the molten metal. Agglomeration was also due to the density variation of reinforcement a due to poor wettability of SSP in the molten base metal pool. Few micro holes could also be observed from the image due to the evolution of carbon dioxide bubbles from the cast surface. When

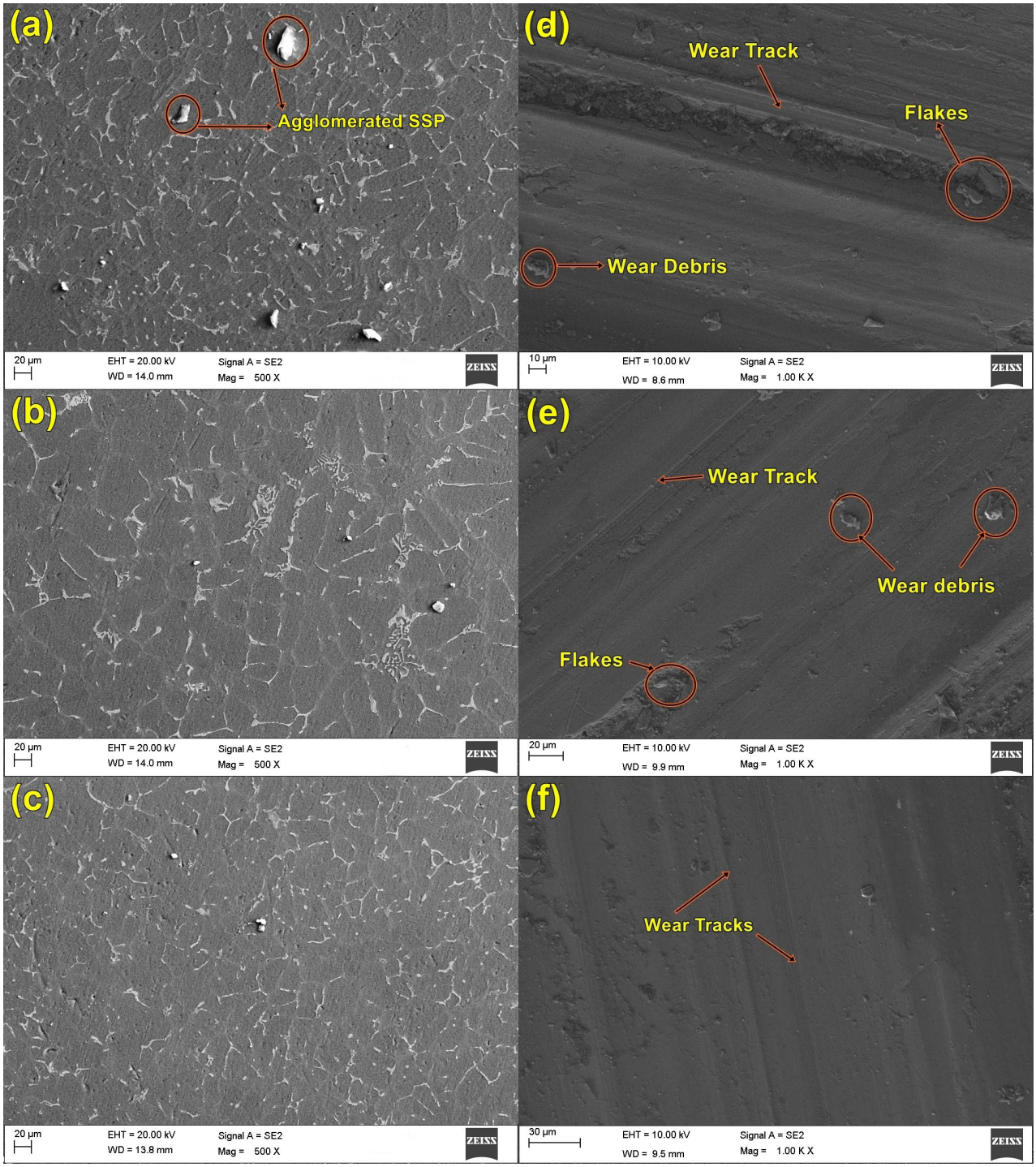

Fig. 6. SEM morphology of AA2219-SSP composites before wear (a) 1 wt. % SSP, (b) 2 wt. % SSP, (c) 3 wt. % SSP, after wear (d) 1 wt. % SSP, (e) 2 wt. % SSP, (f) 3 wt. % SSP

this specimen was subjected to wear, the agglomerates of SSP had undergone wear at the first instant and was converted to wear debris as shown in Fig. 6(d). Due to this, the matrix was left unshielded and so it had undergone a deep wear resulting in formation of deep wear tracks and a significant amount of flakes had also formed. The phenomenon of wear in this study is the adhesive wear since a minimal quantity of material transfer occurred in between the wear pin and the counterfacing disc.

Fig. 6(b) depicts the SEM micrograph of AA2219-SSP composites with 2 wt. % of SSP before subjecting to wear tests which exhibits relatively lower agglomeration when compared with the previous sample. Formation of dendritic structures at the interface could be observed from the figure which depicts the non-uniform cooling of the molten metal and this is attributed to the difference in solidification of the matrix and the reinforcement. Wear surface morphology of this specimen is shown in Fig. 6(e). It could be noticed from this image that the formation of flakes and wear debris were relatively lesser due to the reduced agglomeration of the reinforcement. Wear resistance of this sample was also relatively higher which could be observed from the specific wear rate value in TABLE 7. Wear tracks could be observed in the image but they are shallow.

Fig. 6(c) denotes the SEM micrograph of AA2219-SSP composites with 3 wt. % of SSP. Meagrely agglomerated reinforcement could be noticed from the image which depicts the homogenous dispersion of SSP within AA2219 matrix. This could be attributed to the adequacy of the reinforcement content present in the solid solution. Formation of dendritic structures has also considerably reduced denoting the increase in compatibility between matrix and reinforcement. Wear track morphology of this specimen is shown in Fig. 6(f) and from this image it could be noted that the formation wear debris and flakes were very minimum. Increases interfacial adhesion between the matrix and the reinforcement resulted in shallow wear tracks and the SSP particles shielded the softer AA2219 matrix from wear. In this case, adhesive wear had become abrasive wear which could be evidently witnessed from shallow wear tracks. From all the above discussions, it could be stated that AA2219 composites containing 3 wt. % of SSP performed better in wear test and can be considered for any contact applications of aluminium alloys.

4. Conclusions

Aluminium alloy 2219 reinforced with SSP in weight fractions of 1, 2 and 3 % were prepared by using stir casting process. Characterization of SSP powders by XRD and composite samples by EDS, mechanical properties such as hardness and compressive strength were evaluated, tribological property was determined using wear tests and the surface morphology of the composites were analyzed using SEM. Following conclusion could be coined out from the above experimental study:

- XRD peaks of sea shell powders depicted that calcium carbonate (77%) and calcium hydroxide (59%) were the major constituents of sea shell powder with rhombohedral and hexagonal structures respectively. Particle size of used sea shell powders were calculated using Williamson-Hall synthesis method and was found to be 15.7 microns. EDS spectra of cast samples showcased that the formation of secondary elements was minimum in all the samples which could be ascertained from the elemental presence in each composite ample.
- Mechanical properties of AA21 composites were found to be maximum at 3 wt. % of SSP. The samples exhibited 41% higher hardness and 20% higher compressive strength when compared with the unreinforced base metal.
- Mechanical properties of the AA2219 composites with bio-ceramic reinforcement were found to be higher than the AA2219 composites with alumina reinforcement which suggests that bio based sea shell powders could be a potential and equivalent alternative for the synthetic ceramics.
- Wear resistance of AA2219 composites containing 3 wt. % of SSP was found to higher than all other samples. Specific wear rate and coefficient of friction values were found to be 35% and 64% higher than the unreinforced AA2219 samples thus portraying the significance of reinforcement addition into softer AA2219 matrix.
- Surface morphology of the specimen exhibited few notable aspects before wear such as agglomeration and dendritic structure formation which were high for the sample with 1 wt. % of SSP and low for the sample with 3 wt. % of SSP. After subjecting to wear, the specimens were found to exhibit flakes, wear debris and wear tracks. All these were lower for the samples with 3 wt. % of SSP denoting the better compatibility between matrix and the reinforcement.

Hence, from all the above discussion, it could be stated that AA2219 with 3 wt. % of sea shell powders outperformed its counterparts in all respects and this composition is applicable for many aluminium alloy based engineering applications such as clutches, piston and brake pad.

REFERENCES

[1] L. Rajeshkumar, A. Saravanakumar, V. Bhuvaneswari, G. Gokul, D.D. Kumar, M.J. Karunan, Mater Today-Proc. **27**, 2645-2649 (2020). DOI: https://doi.org/10.1016/j.matpr.2019.11.087

[2] M.K. Surappa, Aluminium matrix composites: Challenges and opportunities, Sadhana-Acad. P. Eng. S. **28**, 319-334 (2003).

[3] A. Baradeswaran, A.E. Perumal, Compos. Part B-Eng. **54**, 146-152 (2013).

[4] L. Rajeshkumar, A. Saravanakumar, V. Bhuvaneswari, M.P. Jithin Karunan, N. Karthick raja, P. Karthi, AIP Conf. Proc. **2207**, 020005 (2020). DOI: https://doi.org/10.1063/5.0000042

[5] G. Moona, R.S. Walia, V. Rastogi, R. Sharma, Mater. Res. Express **6**, 1165d5 (2019).

[6] B.S. Yigezu, M.M. Mahapatra, P.K. Jha, Miner. Mater. Charac. Eng. **01**, 124-130 (2013).

[7] L.R.K. Rajeshkumar, Int. J. Eng. Res. Technol. **6**, 3-8 (2018).
[8] K. Alaneme, A. Aluko, Sci. Iran. **19**, 992-996 (2012).
[9] P.K. Rohatgi, JOM. **46** 55-59 (1994).
[10] B. Mathur, P. Kumar, Tech. Rese. Sci. Special. 1-6 (2020).
[11] L Rajeshkumar, A. Saravanakumar, Particul. Sci. Technol. **38**, 228-235 (2019).
DOI: https://doi.org/10.1080/02726351.2018.1526834
[12] A. Saravanakumar, S. Sivalingam, L.R. Kumar, Mater. Today-Proc. **5**, 8321-8327 (2018).
[13] M.O. Bodunrin, K.K. Alaneme, L.H. Mater. Res. Technol. **4**, 434-445 (2015).
[14] S. Dharmalingam, R. Subramanian, K.S. Vinoth, B. Anandavel, Mater. Eng. Perform. **20** (8), 1457-1466 (2010).
[15] A. Saravanakumar, L. Rajeshkumar, D. Balaji et al., Arab. J. Sci. Eng. **45**, 9549-9557 (2020).
DOI: https://doi.org/10.1007/s13369-020-04817-8
[16] K.K Alaneme, M.O. Bodunrin, A.A. Awe, Engi. Sci. **30**, 96-103 (2018).
[71] N.V. Murthy, A.P. Reddy, N. Selvaraj, C.S.P. Rao, IOP Conf. Ser.-Mat. Sci. **149**, 012106 (2016).
[18] L. Natrayan, M.S. Kumar, K.P. Alanikumar, Mater. Res. Express. **5**, 066516 (2018).
[19] Sharma, Pardeep, Satpal Sharma, Dinesh Khanduja, Asian Ceram. Soc. **3**, 3, 240-244 (2015).
[20] V. Mohanavel, K. Rajan, K.R. Senthilkumar, Appl. Mech. Mater. **787**, 583- 587 (2015).
[21] K.M. Shorowordi, T. Laoui, A.S.M.A. Haseeb, J.P. Celis, L. Froyen, Mater. Proc. Technol. **142**, 738-743 (2003).
[22] A. Saravanakumar, R. Saravanakumar, S. Sivalingam, V. Bhuvaneswari, Int. J. Mech. Prod. Eng. Research Dev. **8** (8), 393-399 (2018).
[23] S.A. Sajjadi, H.R. Ezatpour, H. Beygi, Mater. Sci. Eng. A, **528**, 8765-8771 (2011).
[24] H. Kala, K.K.S. Mer, S. Kumar, Procedia Mater. **6**, 1951-1960 (2014).
[25] V. Bhuvaneswari, L. Rajeshkumar, D. Balaji, R. Saravanakumar, Solid. State Technol. **63** (5), 4552-4560 (2020).
[26] E.C. Nwanji, P.O. Babalola, Mater. Sci. Eng. **413**, 012043. (2018).
[27] L. Rajeshkumar, K.S. Amirthagadeswaran, Materiali in Tehnologije **53**, 57-63. (2019).
DOI: https://doi.org/10.17222/mit.2018.122
[28] S.S. Irhayyim, H.S. Hammood, A.D. Mahdi, AIMS Mater. Sci. **7**, 103-115 (2020).
DOI: https://doi.org/10.3934/matersci.2020.1.103
[29] L. Rajeshkumar, R. Suriyanarayanan, K. Shree Hari, S. Venkatesh Babu, V. Bhuvaneswari, M.P. Jithin Karunan, IOP Conf. Ser.: Mater. Sci. Eng. **954**, 012008 (2020).
DOI: https://doi.org/10.1088/1757-899X/954/1/012008
[30] T. Adithiyaa, D. Chandramohan, D.T. Sathish, Mater. Today: Proc. **21**, 1000-1007 (2020).
DOI: https://doi.org/10.1016/j.matpr.2019.10.051
[31] A. Karthik, R. Karunanithi, S.A. Srinivasan, M. Prashanth, Mater. Today: Proc. **27**, 2574-2581 (2020).
DOI: https://doi.org/10.1016/j.matpr.2019.10.143
[32] V. Bhuvaneswari, L. Rajeshkumar, K. Nimel Ross, J. Mater. Res. Technol. 15, 2802-2819 (2021).
DOI: https://doi.org/10.1016/j.jmrt.2021.09.090